

Primljen / Received: 18.7.2023.

Ispravljen / Corrected: 4.3.2024.

Prihvaćen / Accepted: 25.3.2024.

Dostupno online / Available online: 10.4.2024.

Investigation of the transverse internal force of a box girder using the energy variational principle

Author:



Assoc.Prof. **Zhaonan Wang**, PhD. CE
Lanzhou City University, Lanzhou China
Department of Civil Engineering
524299845@qq.com

Corresponding author

Research Paper

Zhaonan Wang

Investigation of the transverse internal force of a box girder using the energy variational principle

This study investigated the transverse internal force of a box girder with a trapezoidal cross-section under eccentric loading. The effects of the box girder distortion and frame shear difference on the transverse internal force were considered. An energy variation method based on the minimum potential energy principle was adopted for transverse internal force analysis of the frames. The variable shear difference of the top slab was considered an unknown quantity, and a fourth-order governing differential equation was established. The transverse bending moment of the frame was obtained by solving for the shear difference. Two examples were used to verify the proposed method and analyse the differences between the transverse internal force results calculated using different methods. The effect of the distribution of the box-girder distorted transverse bending moment on each slab was investigated for various stiffness ratios. The results showed that the transverse internal force of the box girder calculated using the proposed method agreed well with the finite element results, with a maximum error of less than 9.68%. When the stiffness ratio of the box girder increased, the distribution of the distorted transverse bending moment on the top slab increased, whereas that on the bottom slab decreased.

Key words:

bridge engineering, transverse internal force, energy variational method, box girder with a trapezoidal cross-section, distortion

Prethodno priopćenje

Zhaonan Wang

Ispitivanje poprečne unutarnje sile sandučastog nosača primjenom principa varijacije energije

U ovom je radu ispitana poprečna unutarnja sila sandučastog nosača trapeznog presjeka pod ekscentričnim opterećenjem. Proučeno je kako distorzija sandučastog nosača, ali i razlika u posmiku okvira utječu na poprečnu silu. Za analizu poprečnih unutarnjih sila okvira usvojena je metoda varijacije energije koja se temelji na principu minimalne potencijalne energije. Varijabilna posmična razlika gornje ploče smatrana je nepoznatom veličinom te je utvrđena diferencijalna jednadžba četvrtoga reda. Poprečni moment savijanja okvira dobiven je na temelju razlike u posmiku. Za provjeru predložene metode i analizu razlika između rezultata poprečne unutarnje sile izračunanih različitim metodama primijenjena su dva primjera. Učinak distribucije iskrivljenoga poprečnog momenta savijanja sandučastog nosača na svakoj ploči ispitan je za različite omjere krutosti. Rezultati su pokazali da se poprečna unutarnja sila sandučastog nosača izračunana predloženom metodom podudara s rezultatima konačnih elemenata, s maksimalnom pogreškom manjom od 9,68%. Kad se povećao omjer krutosti sandučastog nosača, distribucija iskrivljenoga poprečnog momenta savijanja na gornjoj se ploči povećala, a na donjoj ploči smanjila.

Ključne riječi:

mostogradnja, poprečna unutarnja sila, metoda varijacije energije, sandučasti nosač trapeznog presjeka, distorzija

1. Introduction

Recently, box girder designs tend to be thin-walled with fewer diaphragms. Under eccentric loading, owing to the influence of the box girder distortion, the calculation of the box girder transverse internal force becomes complex. The transverse bending moment of a box girder is the most important component of the transverse internal force and a key aspect that must be considered when designing a bridge. Inaccurate calculations of transverse bending moments are one of the causes of longitudinal cracks at the junction of the box girder web and top slab.

Several scholars have investigated the accurate calculation of the box girder transverse internal forces. Stefanou et al. [1] considered the influence of distortion on the calculation of transverse internal forces of box girders. Jia et al. [2], Zhao et al. [3,4], and Li et al. [5] studied the transverse internal forces of corrugated steel web box girders using a frame analysis method. Wang et al. [6] proposed an improved frame-analysis method and studied the transverse internal force of a box girder with inclined webs. Chithra et al. [7] used a Simple Frame Analysis (SFA) method to analyse the transverse internal force of a single-box double-cell box girder. The results were calculated and compared with those obtained using a three-dimensional finite-element program. Kurian et al. [8, 9] analysed the insufficiencies of the SFA method and the impacts of a cantilever plate and vehicle load on the transverse bending moment. Rambo-Roddenberry et al. [10] used the finite element method to analyse the transverse internal forces of box girders affected by guardrails. Zheng et al. [11] studied the transverse internal forces in curved box-girder bridges. Guo et al. [12] calculated the transverse internal forces of rectangular and trapezoidal box girders using a frame analysis. Zhong et al. [13] used the finite element method to calculate and analyse the transverse internal force of a box girder. Zhang et al. [14] conducted an experimental study on the lateral stress performance of a prefabricated segmented corrugated steel-web composite box-girder bridge. Resupero et al. [15] developed an analytical model that considered the relationship between longitudinal shear deformation and transverse bending deformation to apply transverse internal force information to the transverse reinforcement design of box girders. The influence of the box girder distortional deformation on the transverse bending moment calculations cannot be ignored, because its magnitude changes the transverse bending moment distribution of each plate. Wang et al. [16] considered the influence of distortion when using a frame analysis method to study the transverse internal forces of single-box double-cell box girders with corrugated steel webs. To study box girder distortion related to transverse internal forces, Zhang et al. [17] studied the distortion of a trapezoidal box girder using a method similar to that used to study torsion and analysed the influence of the parameters on the distortion.

Xu et al. [18] used a generalised coordinate method to study the distortion of box girders. The calculated theoretical values were generally verified using the finite element method. Ji et al. [19] proposed a bridge finite element model modification method based on the response surface method and Fmincon algorithm. This significantly improves the finite element calculation accuracy of the transverse internal force of a box girder.

Research on the transverse internal forces of box girders discussed above was primarily based on frame analysis and finite element methods. In this study, a vertical eccentric load acting on a box girder was decomposed into positive and antisymmetric loads, which not only considered the box girder distortion but also the influence of the frame shear difference on the calculation of the transverse internal force. Using the energy variational method, a fourth-order control differential equation was established. Taking the shear difference on the top slab of the frame, $T(z)$, as the unknown quantity, the frame bending moment caused by the shear difference can be obtained. Finally, the superposition of the bending moments generated by the positive and antisymmetric loads determines the final transverse internal force of the box girder. The effects of stiffness ratio change on the box-girder distorted transverse bending moment were also studied.

2. Assumptions and analysis models

First, a simply supported box girder with a trapezoidal cross-section of equal height was considered, as shown in Figure 1. A vertical eccentric uniformly distributed load $P(z)$ acts on the box girder; for convenience, it is simply referred to as P in this paper. A beam segment of unit length was cut from the middle of the simply supported beam span. Its top slab, bottom slab, web, and other plates formed a closed frame, as shown in Figure 2.

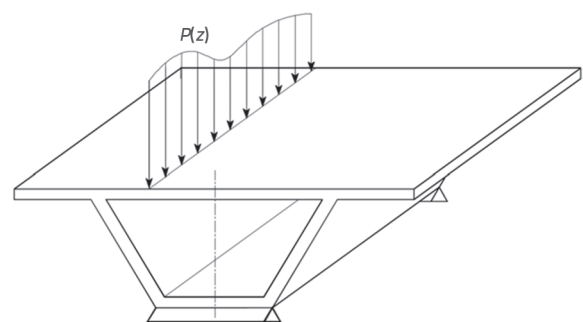


Figure 1. Simply-supported box girder and its distributed load

In Figure 2, a_1 , a_2 , a_3 , and a_4 represent the widths of the left web, bottom slab, right web, and top slab, respectively, d is the width of the cantilever plate, t_1 , t_2 , t_3 , and t_4 are the thicknesses of the left web, bottom slab, right web, and top slab, respectively, and h is the beam height. $I_1 = I_3$, I_2 , and I_4 represent the out-of-plane moments of inertia of the plate elements and can be calculated

using $I_i = t_i^3/[12(1-\mu^2)]$, where $i = 1, 2, 4$, and μ is the Poisson's ratio. The coordinate system is the right-hand coordinate system.

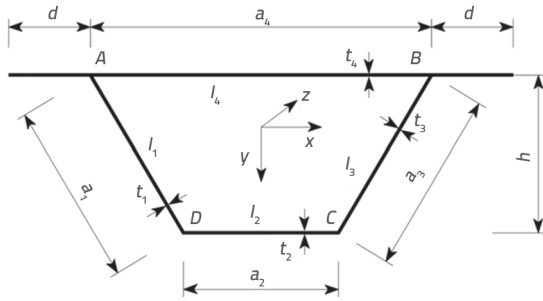


Figure 2. Cross-section of trapezoidal box girder

This frame was taken as the research object, and three primary assumptions were made [6, 16]:

1. The transverse deformation of each plate constituting the frame was ignored, that is, the circumference of the box section was considered incompressible, and there was no transverse strain.
2. When the box girder was distorted, the plates that composed the box section were considered as the cross-section of each longitudinal plate girder, which satisfied the plane section assumption.
3. The influence of the thickness of each box girder plate on warping was ignored, that is, the shear stress and warping normal stress were uniformly distributed along the wall thickness.

To study the transverse internal force of the box girder, the eccentric load applied to the top plate of the box girder was decomposed into positive and antisymmetric loads, as shown in Figure 3, where a represents the distance between the load positions and the edge of the top plate and e is the distance between the load components acting on the top slab.

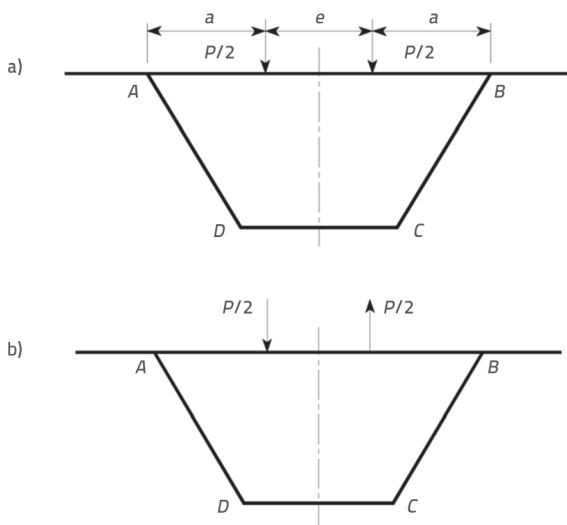


Figure 3. Load decomposition on frame: a) positive symmetric load; b) antisymmetric load

The transverse internal force of a frame experiencing a positive symmetric load can be calculated by first adding the support, removing the support, and replacing it with the reverse bearing force. Finally, the results are superimposed to obtain the transverse internal force of the frame under a positively symmetric load. The bending moment of the frame is extremely small under a reverse bearing force; therefore, it is generally ignored. Because the load had positive symmetry, no transverse bending moment was generated by frame distortion. The transverse internal force generated by a positive symmetric load was calculated using the finite element method or structural mechanics method.

The transverse internal force of the frame under an antisymmetric load was also calculated by first adding the support, then removing the support, and replacing it with the reverse bearing force. In addition to the antisymmetric load, an unknown shear difference, $T(z)$, also acted on each plate of the supported frame; this shear difference is referred to as T in this paper. The loading effects are shown in Figure 4. The frame bending moment was generated by the antisymmetric load $P/2$ and shear difference T . In this figure, T_s , T_x , and T_h represent the shear differences in the top, bottom, and web slabs, respectively. When the shear difference acts on the frame alone, T_s causes the frame to move laterally and generate an internal force; therefore, in this study, the unknown shear difference T refers only to T .

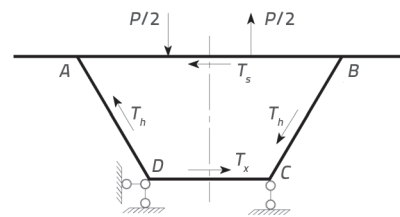


Figure 4. Calculation model for the frame under antisymmetric load

To calculate T , the energy variational principle is used to construct a differential equation with T as an unknown quantity. This was performed to solve for the frame bending moment caused by the shear difference in the top slab. The frame bending moment caused by the antisymmetric load, $P/2$, can be calculated using the structural mechanics method or the finite element method. To establish this differential equation, the relationship between the horizontal displacement of the frame in the x -direction and the antisymmetric load, shown in Figure 4, was determined.

3. Horizontal displacement of the supported frame under the antisymmetric load

3.1. Frame internal force and horizontal displacement caused by the shear difference T

The bending moment diagram of the frame caused by shear difference T indicates antisymmetry about the y -axis, as shown in Figure 5.

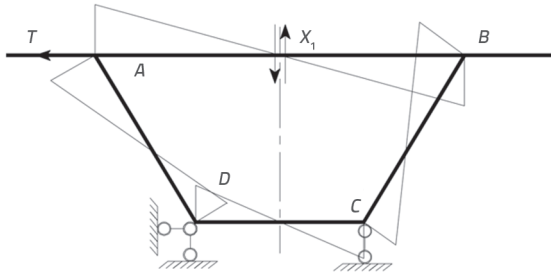


Figure 5. Frame-bending moment caused by the shear difference

The bending moment M_A of point A in Figure 5 is equal to $a_4 X_1 / 2$, and the bending moment M_D of point D is equal to $(a_2 X_1 - hT) / 2$, where

$$X_1 = \left[\frac{a_1(a_4 + 2a_2)}{l_1} + \frac{a_2^2}{l_2} \right] \frac{h}{\Gamma} T \tag{1}$$

$$\Gamma = \frac{a_4^3}{l_4} + \frac{a_2^3}{l_2} + \frac{2a_1(a_2^2 + a_4^2 + a_2 a_4)}{l_1}$$

If $X_1 = \eta_1 Th$, then η_1 can be obtained by comparing Eq.(1). X_1 represents the antisymmetric unknown force on the top slab of the basic system when solving for the frame bending moment caused by the shear difference. Through graph multiplication, the horizontal displacement, $\Delta_T(z)$, of point B of the frame was calculated using Eq. (2):

$$\Delta_T(z) = \left[\frac{a_1 \eta_1 (2a_2 + a_4) - 2a_1}{l_1} + \frac{a_2 (\eta_1 a_2 - 1)}{l_2} \right] \frac{h^2 T}{12E} \tag{2}$$

Eq. (2) can be rewritten as $\Delta_T(z) = TK_T$, where K_T is obtained from Eq. (2), where E is the elastic modulus of the plate.

3.2. Frame internal force and horizontal displacement caused by the antisymmetric load P/2

A bending moment diagram of the frame caused by the antisymmetric load $P/2$ indicates antisymmetry about the y -axis, as shown in Figure 6.

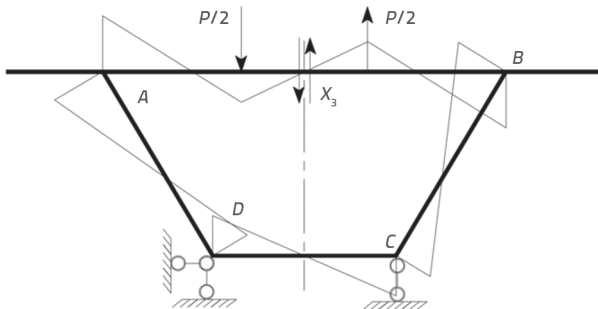


Figure 6. Frame bending moment caused by the antisymmetric load

The bending moment, M_A , at point A in Figure 6 is equal to $(Pa_4 X_3) / 2$, and the bending moment, M_D , at point D is equal to $[2a_2 X_3 - (a_2 - a_4 + 2a)P] / 4$. X_3 , which was calculated using Eq. (3) was used to calculate the antisymmetric unknown force on the top slab of the basic system when determining the frame bending moment under an antisymmetric load $P/2$.

$$X_3 = \left[\frac{a_1(a_2 a_4 - 6a a_2 - 6a a_2 + a_4^2 - 2a_2^2)}{2l_1} + \frac{a_2^2(a_2 - a_4 + 2a)}{2l_2} + \frac{a^2(3a_4 - 2a)}{l_4} \right] \frac{P}{\Gamma} \tag{3}$$

If $X_3 = \eta_3 P$, then η_3 can be obtained from Eq. (3). If $X_1 = \eta_1 Th$, $X_3 = \eta_3 P$ and T represents the unit force, then the horizontal displacement, $\Delta_p(z)$, of point B of the frame caused by $P/2$ can be expressed by Eq. (4):

$$\Delta_p(z) = \frac{Ph}{12E} \left\{ \eta_1 \eta_3 \left[\frac{2a_1(a_4^2 - a_2^2)}{l_1} - \frac{a_2^3}{l_2} + \frac{a_4(6a a_4 - 4a^2 - a_2^2)}{l_4} \right] + \eta_1 \left[\frac{a_2^2(a_2 - a_4 + 2a)}{2l_2} + \frac{a^2(2a - 3a_4)}{l_4} + \frac{a_1(a_4 - 2a_2 - 6a)(a_4 - a_2)}{2l_1} \right] + \eta_3 \left[\frac{a_1(a_4 + 2a_2)}{l_1} + \frac{a_2^2}{l_2} \right] + \frac{a_1(a_4 - 3a - a_2)}{l_1} + \frac{a_2(a_4 - 2a - a_2)}{2l_2} \right\} \tag{4}$$

Eq. (4) can be rewritten as $\Delta_p(z) = PK_p$, and K_p can be obtained from Eq. (4).

The analysis indicated a relationship between the horizontal displacement of the frame under $P/2$ and shear difference T , as shown in Figure 4. This relationship is expressed by Eq. (5):

$$\Delta(z) = \Delta_p(z) + \Delta_T(z) \tag{5}$$

Eq. (5) can also be written as $\Delta(z) = PK_p + TK_T$, and differentiating this expression twice yields Eq. (6):

$$\Delta''(z) = P''K_p + T''K_T \tag{6}$$

4. Total potential energy of the frame and establishment of the differential equation

4.1. Transverse bending strain energy, Π_w

Under the combination of the antisymmetric load, $P/2$, and the shear difference, T , the transverse bending strain energy, Π_w , of a box girder of unit length was composed of M_p and M_T , which represent the bending moments of the supported frame under $P/2$ and T , respectively. The transverse bending strain energy of the supported frame under an antisymmetric load was calculated as follows.

4.1.1. Transverse bending strain energy of the frame under antisymmetric load $P/2$

Self-multiplying the frame moment diagram in Figure 6 and taking half the value yields Eq. (7):

$$\int_s \frac{M_r^2}{2EI} ds = \frac{P^2}{12E} \left\{ \eta_3^2 \left[\frac{4aa_4(2a-a_4)+a_4^3}{2I_4} + \frac{a_1(a_2^2+a_2a_4+a_4^2)}{I_1} + \frac{a_2^3}{2I_2} \right] + \eta_3 \left[\frac{a_2^2(a_4-a_2-2a)}{2I_2} - \frac{a^2(a_4+2a)}{I_4} + \frac{a_1(a_4+2a_2)(a_4-a_2)-6aa_1(a_2+a_4)}{2I_1} \right] + \frac{a^3}{I_4} + \frac{a_1(a_2-a_4)(a_2-a_4+6a)+12aa_1a^2}{4I_1} + \frac{a_2(a_2-a_4)(a_2-a_4+4a)+4a^2a_2}{8I_2} \right\} \quad (7)$$

The right side of Eq. (7) can be rewritten as $P^2 K_{mp}$, where K_{mp} is obtained from Eq. (7). I represents the out-of-plane moment of inertia of each plate, and the integral path s is the perimeter of the box section.

4.1.2. Transverse bending strain energy of frame under shear difference T

Self-multiplying the frame moment diagram in Figure 5 and taking half the value yields Eq. (8):

$$\int_s \frac{M_T^2}{2EI} ds = \frac{T^2 h^2}{12E} \left\{ \eta_1^2 \left[\frac{a_4^3}{2I_4} + \frac{a_2^3}{2I_2} + \frac{a_1(a_4^2+2a_2^2-2a_2a_4)}{2I_1} \right] + \frac{a}{2I_2} + \frac{a_1}{I_1} + \eta_1 \left[\frac{a_1(a_4-2a_2)}{I_1} - \frac{a_2^2}{I_2} \right] \right\} \quad (8)$$

The right side of Eq. (8) can be rewritten as $T^2 K_{mT}$, where K_{mT} is obtained from Eq. (8).

4.1.3. Transverse bending strain energy of the frame caused by a combination of antisymmetric load P/2 and shear difference T

The bending moment diagrams in Figure 5 and 6 are multiplied to obtain Eq. (9):

$$\int_s \frac{M_1 M_2}{EI} ds = \frac{TPh}{12E} \left\{ \eta_1 \eta_3 \left[\frac{a_4(6aa_4-4a^2-a_4^2)}{I_4} + \frac{a_2^3}{I_2} - \frac{a_1(4a_2^2-2a_2^2-a_2a_4)}{2I_1} \right] + \eta_1 \left[\frac{a^2(2a-3a_4)}{I_4} - \frac{a_2^2(a_2-a_4+2a)}{2I_2} - \frac{a_1(6a-a_4+2a_2)(a_4-a_2)}{2I_1} \right] + \eta_3 \left[\frac{a_1(a_4+4a_2)}{2I_1} - \frac{a_2^2}{I_2} \right] + \frac{a_2(a_2-a_4+2a)}{2I_2} - \frac{a_1(3a+a_2-a_4)}{I_1} \right\} \quad (9)$$

The right side of Eq. (9) can be rewritten as TPK_{mPT} , where K_{mPT} is obtained from Eq. (9). The transverse bending strain energy of the frame can be expressed using Eq. (10):

$$\Pi_w = P^2 K_{mp} + T^2 K_{mT} + TP K_{mPT} \quad (10)$$

4.2. External load potential energy, Π_p

Angular displacement, $\theta(z)$, occurred in the box girder cross-section under the antisymmetric loading. It is referred to as θ in this paper. The angular displacement, θ , of the box girder cross-section can be calculated using Eq. (11):

$$\theta = \int_s \frac{(M_p + M_T) M_0}{EI} ds \quad (11)$$

where M_0 represents the frame bending moment generated by the unit moment acting on the mid-span of the top slab of the frame, as shown in Figure 7.

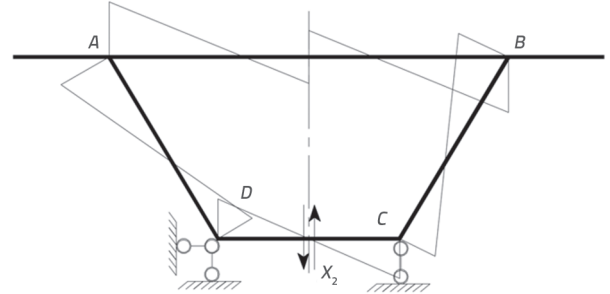


Figure 7. Frame-bending moment caused by the unit moment

The bending moment, M_A , at point A in Figure 7 is equal to $a_4 X_2 / 2 + (a_4 - a_2) / (2a_2)$, and M_D is equal to $a_2 X_2 / 2$. X_2 represents the antisymmetric unknown force on the bottom slab in the basic system when solving for M_0 and it can be expressed by Eq. (12):

$$X_2 = \frac{a_1(2a_4^2 - a_2a_4 - a_2^2)}{a_2 I_1 \Gamma} + \frac{a_4^2(4a_4 - 5a_2)}{2a_2 I_4 \Gamma} \quad (12)$$

Let $X_2 = \eta_2 P$, Substituting $X_3 = \eta_3 P$, $X_1 = \eta_1 T$, $X_2 = \eta_2$ into Eq. (11), we obtain an expression for θ :

$$\theta = \frac{P}{24E} \left\{ [2a_4 \eta_2 \eta_3 (4a^2 - 6aa_4 + a_4^2) + 2a^2 \eta_2 (3a_4 - 2a) + 2a^2 (3a_4 - 3a_2 - 2a) + a_4 \eta_3 \left(\frac{8a^2}{a_2} + \frac{2a_4^2}{a_2} - \frac{12aa_4}{a_2} + 12a - 3a_4 \right) \frac{1}{I_4} + [(6a - a_4 - 4a_2 \eta_3) \frac{\eta_2 + 1}{a_2} + (1 - 2\eta_3)(2\eta_2 + 1)) \frac{a_1(a_4 - a_2)}{I_1} + \frac{a_2^2 \eta_2 (2a_2 \eta_3 - 2a + a_4 - a_2)}{I_2} \right\} + \left\{ \frac{a_1^2 \eta_1 (3a_2 - 2a_2 - 2a_2 a_1 \eta_2)}{2a_2 I_4} + \frac{a_2^2 \eta_2 (1 - a_2 \eta_1)}{I_2} - \frac{1}{I_1} [2a_1 \eta_1 \eta_2 (a_4^2 - a_2 a_4 + a_2^2) + a_1 \eta_2 (a_4 - 2a_2) + \frac{a_1(a_4 - a_2)(1 + 2\eta_1 a_4 - \eta_1 a_2)}{a_2}] \right\} \frac{hT}{12E} \quad (13)$$

Eq. (13) can be rewritten as $\theta = PK_{\theta p} + TK_{\theta T}$, where $K_{\theta p}$ and $K_{\theta T}$ can be obtained from Eq. (13). Thus, the external load potential energy on the frame is equal to $\Pi_p = -(P^2 K_{\theta p} + PK_{\theta T})/2$.

4.3. Longitudinal warping strain energy, Π_q

The warping strain energy of a box girder of unit length can be expressed by $\Pi_q = \int_{\Omega} \frac{\sigma^2}{2E} d\Omega$, and the integral of Ω represents the cross-section of each plate of the box girder. According to the assumptions in this study, the distribution of the warping normal stress on each plate is shown in Figure 8. Ignoring the influence of web warping strain energy, the warping strain energy of the frame is calculated using Eq. (14).

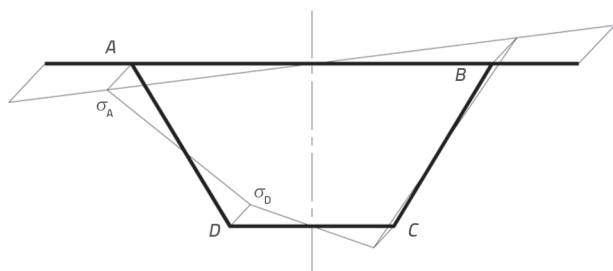


Figure 8. Distribution of distortion-warping normal stress

$$\Pi_q = \frac{[\Delta''(z)]^2 E}{24(a_2 + a_4\beta)^2} [a_2^2 a_4^2 (t_4 a_4 + t_2 a_2 \beta^2) + t_4 d a_2^2 (3a_4^2 + 3a_4 d + d^2)] \quad (14)$$

In Eq. (14), σ_A and σ_D represent the distortion-warping normal stresses at corner points A and D, respectively. If $\beta = \sigma_D / \sigma_A$ and $\Pi_q = K_q [\Delta''(z)]^2$, then K_q can be obtained from Eq. (14). Substituting Eq. (6) into Eq. (14) yields an expression for Π_q , as shown in Eq. (15):

$$\Pi_q = K_q K_p^2 (P'')^2 + 2K_T K_p K_q P'' T'' + K_q K_T^2 (T'')^2 \quad (15)$$

4.4. Establishment and solution of the differential equation

Through the analysis presented above, an equation is obtained for the total potential energy of the frame, which includes the transverse bending strain energy, warping strain energy, and external load potential energy.

$$\Pi = \Pi_w + \Pi_q + \Pi_p \quad (16)$$

Substituting the appropriate expressions into Eq. (16) yields Eq. (17):

$$\Pi = K_q K_T^2 (T'')^2 + 2K_T K_p K_q P'' T'' + T^2 K_{mT} + \frac{2PK_{mPT} - PeK_{\theta T}}{2} T + \frac{2K_{mp} - eK_{\theta T}}{2} P^2 + K_q K_p^2 (P'')^2 \quad (17)$$

According to the Euler equation, the differential equation can be obtained as follows:

$$T'''' K_q K_T + T K_{mT} + \frac{2PK_{mPT} - PeK_{\theta T}}{4} = 0 \quad (18)$$

If $\lambda_1 = \left(\frac{K_{mT}}{4K_q K_T} \right)^{1/4}$, then Eq. (18) can be rewritten as (19):

$$T'''' + 4\lambda_1^4 T = \frac{eK_{\theta T} - 2K_{mPT}}{4K_q K_T} P \quad (19)$$

This differential equation is similar to the flexure differential equation of Beam on Elastic Foundation, and it can be solved using an analogy solution for Beam on Elastic Foundation when

$P(eK_{\theta T} - 2K_{mPT}) / (4K_q K_T)$ is the unit load. The form of the solution as to Eq. (20), where $k = K_{mT} / K_T$. The shear difference, T , of the frame under a unit load can be obtained from Eq. (20), and the result is multiplied by $P(eK_{\theta T} - 2K_{mPT}) / (4K_q K_T)$. Therefore, the shear difference of the supported frame under an antisymmetric load is obtained as follows:

$$T(z) = \frac{\lambda_1 e^{-\lambda_1 z}}{2k} [\cos(\lambda_1 z) + \sin(\lambda_1 z)] \quad (20)$$

The box girder had $T(z) = 0$ at the fixed end, simply supported end with a rigid diaphragm and free end with a rigid diaphragm. After calculating T , the transverse moment of the frame under shear difference can be obtained. By superposition with the transverse bending moment of the frame under antisymmetric load $P/2$, the transverse bending moment of the supported frame under antisymmetric load can be obtained.

5. Distorted transverse bending moment of the frame caused by the antisymmetric reverse bearing force

When calculating the transverse bending moment of the frame under an antisymmetric load, a supporting force was applied to the frame without support. This caused the frame to produce a transverse bending moment owing to distortion. The distortion angle γ , represents the change in the angle between the web and the bottom slab at frame point D. This is used to express the bending moment at the end of each plate. If $M_A = k_1 \gamma$ and $M_D = k_2 \gamma$, with $k_1 = a_4 \eta_1 h^2 / K_T$, $k_2 = (h^2 - a_2 \eta_1 h^2) / K_T$, then the differential equation, which includes γ , can be expressed as:

$$EI_{\omega D} \gamma'''' + EI_R \gamma = P_z F_s \quad (21)$$

In Eq. (21), $EI_{\omega D}$ represents the distortion warping stiffness, EI_R is the lateral frame stiffness, $F_s = a_1(a_2 + a_4) / (2h)$, and P_z represents the supporting force of the supported frame under the antisymmetric load. The solution to this equation is relatively mature, and the details regarding the initial parameter method can be obtained from the references. Therefore, a solution form is not presented in this paper.

After calculating the distorted transverse bending moment of the frame, it was superimposed with the transverse bending moment of the frame with support under the antisymmetric load, as well as with the transverse bending moment of the frame with support under the positive symmetric load. This superposition produces the final transverse bending moment of the frame. Notably, the out-of-plane bending moment of each plate in the frame, which was generated by removing the support and replacing it with the reverse bearing force, must be accounted for when calculating the transverse bending moment of the trapezoidal box girder under the antisymmetric load. However, when calculating the transverse bending moment of a rectangular box girder, an out-of-plane bending moment cannot be generated because of the reverse bearing force acting on the in-plane side of the web.

Therefore, it is not considered. This is the difference between trapezoidal and rectangular box girders when using this method to calculate the transverse bending moment.

6. Numerical examples and a parameter analysis

6.1. Numerical examples

Numerical Example 1: A uniform line load, $P = 1$ kN/m, was applied to a simply supported box girder with a trapezoidal cross-section. Its calculated span, L , was 1.2 m, its material elastic modulus, E , was 2.8 GPa, and its Poisson's ratio, μ , was 0.37. The section dimensions are shown in Figure 9, where the action location of P was 50 mm from point A . The transverse bending moments of corner points A , B , C , and D of the box girder were calculated using the proposed and other methods.

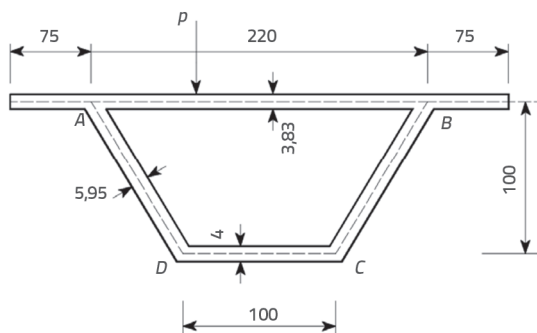


Figure 9. Cross-section of Numerical Example 1 [mm]

Table 1 lists the results obtained using the proposed method. When calculating the transverse bending moment under the antisymmetric load, the antisymmetric reverse bending force caused a bending moment in each plate of the frame (item ③ in Table 1). Ignoring this bending moment causes a large error, particularly regarding the influences of corner points C and D . For a box girder with a rectangular cross-section, this value of the bending moment is zero, whereas, for a box girder with a trapezoidal cross-section, this value of the bending moment cannot be ignored. The frame transverse bending moment diagram for the numerical example is shown in Figure 10. The bending moment calculation points at each corner of the frame and the positive or negative sign of the bending moment are shown in Figure 10.

Rigid support, frame analysis, and finite element methods were also used to calculate the transverse bending moments of the frame for the box girder in Numerical Example 1, and Comparisons of these results with the calculation results of the method proposed in this study are shown in Table 2. The accuracies of the various methods used to calculate the transverse internal force of the box girder differed. The finite-element model calculations used shell-element modelling for this example.

The rigid support method is a simplified and approximate method that does not consider the bending moment generated by the frame distortion effect and produces a large error. The accuracy of the frame analysis method was

Table 1. Transverse bending moment results for Numerical Example 1 calculated using the proposed method

Frame node	A	B	C	D
Frame bending moment caused by positive symmetric loading (with supports) ①	-17.731	-17.731	-1.702	-1.702
Frame bending moment caused by antisymmetric loading (with supports) ②	-11.542	11.542	11.117	-11.117
Frame bending moment caused by antisymmetric loading (without supports) ③	4.754	-4.754	-14.203	14.203
Frame bending moment caused by the shear difference, T ④	-0.073	0.073	0.073	-0.073
Distorted transverse bending moment ⑤	1.474	-1.474	-4.400	4.400
Total frame bending moment (① + ② + ③ + ④ + ⑤)	-23.118	-12.344	-9.115	5.710
All the bending moment values have the units of 10^{-3} kN-m/m.				

Table 2. Comparison of the transverse bending moment results calculated using different methods for Numerical Example 1.

Frame node	A	B	C	D
Frame bending moment calculated using the rigid support method [6, 12] ①	-26.120	-9.518	0.082	-3.441
Frame bending moment calculated using the frame analysis method [6, 12] ②	-22.897	-12.741	-7.763	4.404
Frame bending moment calculated using the proposed method ③	-23.118	-12.344	-9.115	5.710
Frame bending moment calculated using the finite element method ④	-22.068	-12.108	-8.786	5.206
Error 1 [%]: $[(② - ④) / ④] \times 100$	3.76	5.23	-11.64	-15.41
Error 2 [%]: $[(③ - ④) / ④] \times 100$	4.76	1.95	3.74	9.68
All the bending moment values have the units of 10^{-3} kN-m/m.				

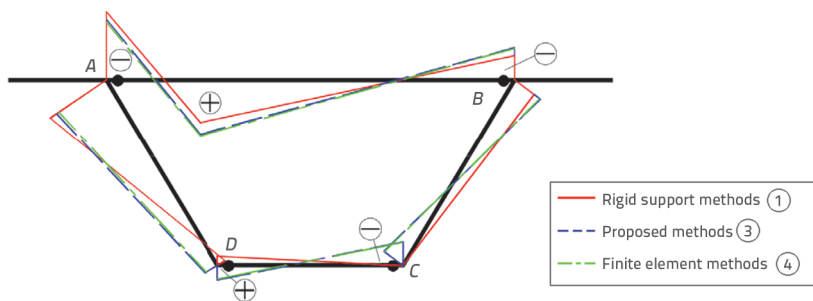


Figure 10. Transverse bending moment results for Numerical Example 1

significantly better because it accounted for the distorted transverse bending moment. However, there were still large errors in the bending moment results for corner points *C* and *D*. The absolute values of these errors were 11.64 % and 15.41 %, respectively. Overall, the results obtained using the proposed method agreed well with the finite element results, and the error between them was relatively small. For example, the absolute values of the bending-moment errors at points *C* and *D* were 3.74 % and 9.68 %, respectively. Although the bending moment error at corner *A* was slightly higher than that obtained using the frame analysis method, the errors at the other corners were smaller, and the overall accuracy was better.

Numerical Example 2: The second numerical example used a double-track ballastless railway track simply supported box girder as the research object. The calculation span was $L = 31.5$ m, elastic modulus was $E = 34.5$ GPa, and Poisson's ratio was $\mu = 0.17$. The dead weight of the structure was 25.0 kN/m³, the live load was converted into a transverse load on the box girder of $P = 27.28$ kN/m², and its transverse distribution width was 2.8 m. The box girder cross-section and load distribution are shown in Figure 11.

The transverse bending moment of the frame caused by an eccentric live load was calculated using the method proposed in this study. Table 3 presents the results of the study. Because the dead load is positively symmetric,

the calculation results are not listed separately. When calculating the transverse bending moment of the frame under the antisymmetric load, the bending moment of each plate (item ③ in Table 3) in the frame without supports caused by the reverse bearing force could not be ignored; for example, the absolute values of the bending moments at points *C* and *D* reached 6.139 kN·m/m. The total bending moment value generated by the live load in Table 3 was added to the value generated by the dead load of the box girder to obtain the overall transverse bending moment of the box girder under both dead and live loads. Table 4 presents the overall transverse bending moment results obtained using different calculation methods. In this example, the finite element calculation model uses shell element modelling.

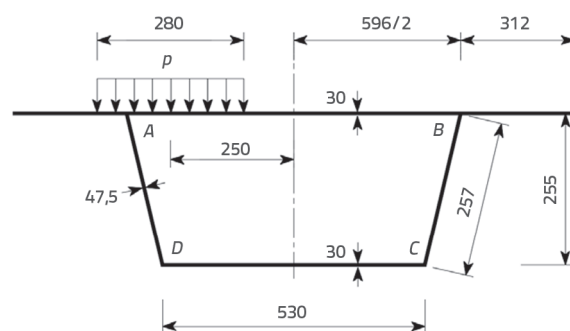


Figure 11. Cross-section of Numerical Example 2 (cm)

Table 4 presents a comparison of the results of several transverse internal force calculation methods. This indicates that the error of the frame analysis method at corner point *D* was 8.26 %, whereas that of the proposed method was 3.10 %. The proposed method exhibits a smaller error and higher accuracy.

Table 3. Transverse bending moments under the live load calculated for Numerical Example 2 using the proposed method

Frame node	A	B	C	D
Frame bending moment caused by positive symmetric loading (with supports) ①	-15.855	-15.855	-0.531	-0.531
Frame bending moment caused by antisymmetric loading (with supports) ②	-11.357	11.357	0.474	-0.474
Frame bending moment caused by antisymmetric loading (without supports) ③	4.986	-4.986	-6.139	6.139
Frame bending moment caused by the shear difference, T ④	-12.500	12.500	12.500	-12.500
Distorted transverse bending moment ⑤	28.830	-28.830	-34.670	34.670
Total frame bending moment (① + ② + ③ + ④ + ⑤)	-5.896	-25.814	-28.366	27.304
All the bending moment values have the units of 10^{-3} kN·m/m.				

Table 4. Comparison of transverse bending moment results calculated using different methods as Numerical Example 2

Frame node	A	B	C	D
Frame bending moment calculated using the rigid support method [6] ①	-316.220	-293.090	-157.340	-157.340
Frame bending moment calculated using the frame analysis method [6] ②	-296.090	-313.220	-181.550	-133.130
Frame bending moment calculated using the proposed method ③	-291.726	-311.644	-180.456	-126.786
Frame bending moment calculated using the finite element method ④	-287.210	-306.050	-171.670	-122.970
Error 1 [%]: $[(② - ④) / ④] \times 100$	3.09	2.34	5.76	8.26
Error 2 [%]: $[(③ - ④) / ④] \times 100$	1.57	1.83	5.12	3.10
All the bending moment values have the units of 10^{-3} kN·m/m.				

6.2. Influence of the stiffness ratio on the distorted transverse bending moment

The parameters that affect the transverse internal force of the box girder include web inclination and height–width ratio. This has already been analysed in detail in the literature [6]. The top slab–web stiffness ratio of the box girder is an important factor affecting the distribution of the transverse internal force on each plate of the box girder. Zhao et al. [3, 4] studied the effect of the linear stiffness ratio on the distribution of the transverse internal force on each plate. The distorted transverse bending moment is an important factor that affects the accuracy of box girder transverse internal force calculations. Therefore, this study focused on analysing the influence of the change in the top slab–web stiffness ratio on the distribution of the distorted transverse bending moment. The stiffness ratio between the top slab and the web was defined as $\xi = t_4^3/t_1^3$ and each box girder plate was made of the same material.

In this section, Case 1 refers to a situation in which the top slab thickness changes and the web thickness remains constant. Case 2 refers to a situation in which the top slab thickness remains constant and the web thickness changes. Based on Numerical Example 2, the numerical values calculated by the frame analysis methods and the influence of a change in the stiffness ratio on the distorted transverse bending moment

were investigated for two sets of working conditions. The distorted transverse bending moments of corner points *B* and *C* of the box girder and those of corner points *A* and *D* were mutually antisymmetric. For this study, the effects of the distorted transverse bending moments at points *A* and *D* were studied for changes in the stiffness ratio, ξ ; these results could reflect the influence of a change in the stiffness ratio on the distribution of the distorted transverse bending moment on each box girder plate.

The results presented in Figure 12 correspond to incremental thickness changes of 0.025 m for the box girder plate. For Case 1, ξ was 0.25, 0.32, 0.40, 0.49, 0.60, 0.72, 0.85, 1.00, 1.17, 1.35, 1.55, and 1.77. The bending moment at corner *A* gradually increased with increases in ξ . The bending moment at corner *D* first gradually increased with an increase in ξ , then decreased gradually. For Case 2, ξ was 0.25, 0.30, 0.35, 0.42, 0.51, 0.63, 0.79, 1.00, 1.30, 1.73, 2.37, and 3.38, respectively. The bending moment at corner *A* gradually increased with an increase in ξ , though when ξ reached 1.73, the bending moment at corner *A* began to decrease. The bending moment at corner *D* decreased gradually as ξ increased.

For both Case 1 and Case 2, the distorted transverse bending moment at corner *A* gradually increased overall with increases in ξ , while the distorted transverse bending moment at corner *D* gradually decreased overall with increases in ξ . The changes at

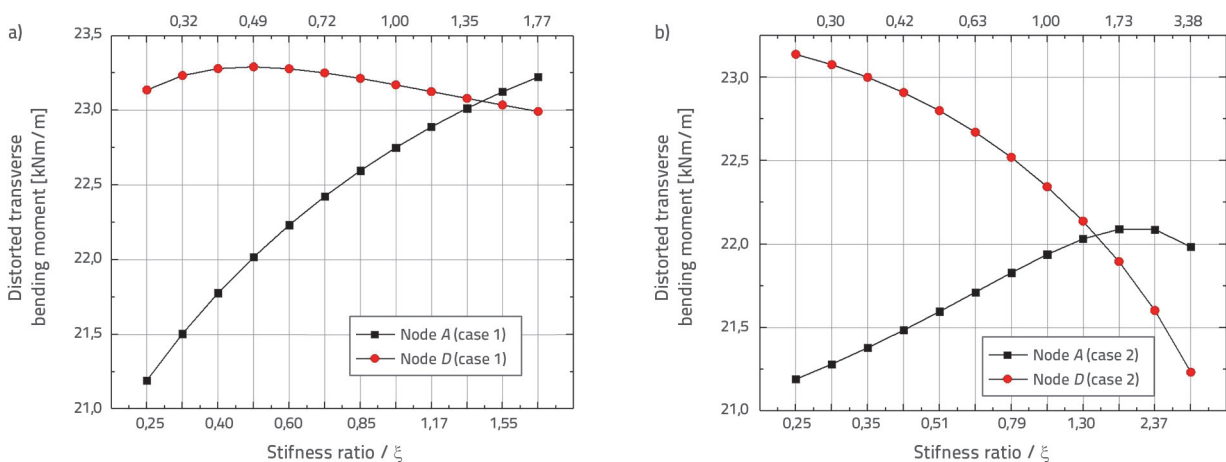


Figure 12. Effects of changes in stiffness ratio on the distorted transverse bending moment: a) Case 1; b) Case 2

corner *A* were more notable in Case 1 than in Case 2, whereas the change trend at corner *D* was the opposite of that at corner *A*. The variation in the stiffness ratio affects the distribution of the bending moment on each plate of the box girder cross-section, and the bending moment distributed for the plate with a larger stiffness is greater than that of the plate with a smaller stiffness. An analysis of the influence of changes in the stiffness ratio on the distorted transverse bending moment can indirectly reflect the influence of changes in the stiffness ratio on the distribution of the transverse internal force on each box girder plate.

7. Conclusions

This study uses the principle of energy variation instead of other conventional methods to calculate the transverse internal force of a thin-walled box girder under eccentric loads. Taking into account the influence of box girder distortion and using the shear difference of the top plate as an unknown quantity in the differential equation, through numerical analysis and parameter research, the following findings were obtained in this study. Unlike considering the horizontal displacement of the top slab of a box girder as an unknown quantity, a fourth-order control differential equation that considered the shear difference of the top slab as an unknown quantity was used to analyse the transverse internal force in this study. The numerical calculation results show that the results of this method are more consistent with those of the finite element method than with the other methods, with a maximum error not exceeding 9.68 %.

The proposed method simultaneously considers the effects of box girder distortion and top slab shear difference on the transverse bending moment under an antisymmetric load. The overall error was small, and the accuracy of the box girder transverse internal force calculations improved.

When using this method to analyse the transverse internal force of a box girder with a trapezoidal cross-section, it is necessary to consider the out-of-plane bending moment of each plate produced by removing the support and replacing it with a reverse bearing force under an antisymmetric load. Otherwise, the error is large, particularly for the transverse bending moment of the bottom slab.

Changes in the stiffness ratio between the top slab and the web of the box girder significantly influenced the distribution of the distorted transverse bending moment on each plate. The bending moment distributed for the plate with larger stiffness was greater than that of the plate with smaller stiffness, and the bending moment change of corner *A* was more notable in Case 1 than in Case 2, whereas the trend of corner *D* was opposite to that of corner *A*. The analysis of the transverse internal force of the box girder presented in this study can provide a reference for future box girder designs.

Acknowledgments

The work described in this paper was supported by grants from the Lanzhou City University Doctoral Research Fund (Grant No. LZCU-BS2022-09). We thank LetPub (www.letpub.com) for linguistic assistance during the preparation of this manuscript.

REFERENCES

- [1] Stefanou, G.D., Dritsos, S., Bakas, G.J.: The effects of additional deformations in box-beam bridges on the longitudinal stresses and transverse moments, *Computers - Structures*, 16 (1983) 5, pp. 613–628, [https://doi.org/10.1016/0045-7949\(83\)90110-4](https://doi.org/10.1016/0045-7949(83)90110-4)
- [2] Jia H.J., Dai H., Zhang J.D.: Research on transverse internal forces in box-girder bridges with corrugated steel webs, *Engineering Mechanics* 31 (2014) 12, pp. 76–81, <https://doi.org/10.6052/j.issn.1000-4750.2013.06.0530>
- [3] Zhao, P., Ye, J.S.: Frame analysis method of transverse internal force in bridge deck of box girders with corrugated steel webs, *Journal of Southeast University(Natural Science Edition)*, 42 (2012) 5, pp. 941–942, <https://doi.org/10.3969/j.issn.1001-0505.2012.05.026>
- [4] Zhao, P., Ye, J.S.: Transverse force study of single-box multichamber with corrugated steel webs, *Journal of Harbin Engineering University*, 39 (2018) 6, pp. 1109–1114, <https://doi.org/10.11990/jheu.201610073>
- [5] Li, Y.L., Yang, B.W., Zhang, J.D.: Transverse moment of PC single box-girder bridge with corrugated steel webs, *Journal of Central South University(Science and Technology)*, 47 (2016) 8, pp. 2802–2808, <https://doi.org/10.11817/j.issn.1672-7207.2016.08.035>
- [6] Wang, Y.S., Zhang, Y.H.: Research on transverse internal force and its parameter influence of thin-walled box girders with inclined webs, *Journal of the China Railway Society*, 39 (2017) 3, pp. 104–110, <https://doi.org/10.3969/j.issn.1001-8360.2017.03.017>
- [7] Chithra, J., Nagarajan, P., Sajith, S.A.: Simplified method for the transverse bending analysis of twin-celled concrete box girder bridges, *Materials Science and Engineering*, 330 (2018) 012118, pp. 1–6, <https://doi.org/10.1088/1757-899X/330/1/012118>
- [8] Kurian, B., Menon, D.: Correction of errors in simplified transverse bending analysis of concrete box-girder bridges, *Journal of Bridge Engineering*, 10 (2005) 6, pp. 650–657, [https://doi.org/10.1061/\(ASCE\)1084-0702\(2005\)10:6\(650\)](https://doi.org/10.1061/(ASCE)1084-0702(2005)10:6(650))
- [9] Kurian, B., Menon, D.: Transverse bending analysis of concrete box girder bridges with flange overhangs. *Structural Engineering(Madra)*, 35 (2008) 3, pp. 173–179.
- [10] Rambo-Roddenberry, M., Kuhn, D., Tindale Jr., R.G.: Barrier effect on transverse load distribution for prestressed concrete segmental box girder bridges, *Journal of Bridge Engineering*, 21 (2016) 04016019, [https://doi.org/10.1061/\(asce\)be.1943-5592.0000814](https://doi.org/10.1061/(asce)be.1943-5592.0000814)

- [11] Zheng, Z.: Calculation method of the continuous rigid-frame curved box girder, *China Journal of Highway and Transport*, 13 (2000) 4, pp. 57–61, <https://doi.org/10.19721/j.cnki.1001-7372.2000.04.013>
- [12] Guo, J.Q., Fang, Z.Z., Zheng, Z.: Design theory of box bridges, Version 2, Beijing: China Communications Press, China, pp. 93–116 (2008).
- [13] Zhong, X.G., Shu, X.J., Zhang, H.Y.: Finite element analysis on transversal frame–effect of prestressed concrete box–girder bridge, *Chinese Journal of Computational Mechanics*, 30 (2013) 4, pp. 549–552, <https://doi.org/10.7511/jslx201304016>.
- [14] Zhang, H., Zheng, H., Wang, M.: Experimental study on transverse mechanical behaviour of precast segmental composite box girder bridge with corrugated steel webs, *Journal of Southeast University(Natural Science Edition)*, 46 (2016) 5, pp. 1070–1075, <https://doi.org/10.3969/j.issn.1001-0505.2016.05.029>
- [15] Recupero, A., Granata, M.F., Culotta, G., Arici, M.: Interaction between longitudinal shear and transverse bending in prestressed concrete box girders *Journal of Bridge Engineering*, 22 (2016) 04016107, [https://doi.org/10.1061/\(asce\)be.1943-5592.0000990](https://doi.org/10.1061/(asce)be.1943-5592.0000990).
- [16] Wang, Z.N., Zhang, Y.H.: Research on transverse internal force of single box double cell composite box girder with corrugated steel webs. *Journal of the China Railway Society*, 41 (2019) 12, pp. 106–112, <https://doi.org/10.3969/j.issn.1001-8360.2019.12.014>
- [17] Zhang, Y.H., Liu, Z.X., Lin, L.X., Zhou, M.D.: Analysis on distortion effect of thin-walled box girders based on principle of stationary potential energy *Journal of Central South University (Science and Technology)*, 47 (2016) 10, pp. 3461–3468, <https://doi.org/10.11817/j.issn.1672-7207.2016.10.024>
- [18] Xu, X., Qiang, S.Z.: Research on distortion analysis theory of thin-walled box girder, *Engineering Mechanics*, 30 (2013) 11, pp. 192–200, <https://doi.org/10.6052/j.issn.1000-4750.2012.07.0554>.
- [19] Ji, W., Shao, T.Y.: Finite element model updating for improved box girder bridges with corrugated steel webs using the response surface method and Fmincon algorithm, *KSCE Journal of Civil Engineering*, 25 (2021) 2, pp. 586–602, <https://doi.org/10.1007/s12205-020-0591-3>